



Lawrence Berkeley Laboratory

UNIVERSITY OF CALIFORNIA

RECEIVED
LAWRENCE
BERKELEY LABORATORY

Materials & Molecular Research Division

NOV 1 1983

LIBRARY AND
DOCUMENTS SECTION

Submitted to the Journal of the American Ceramic
Society

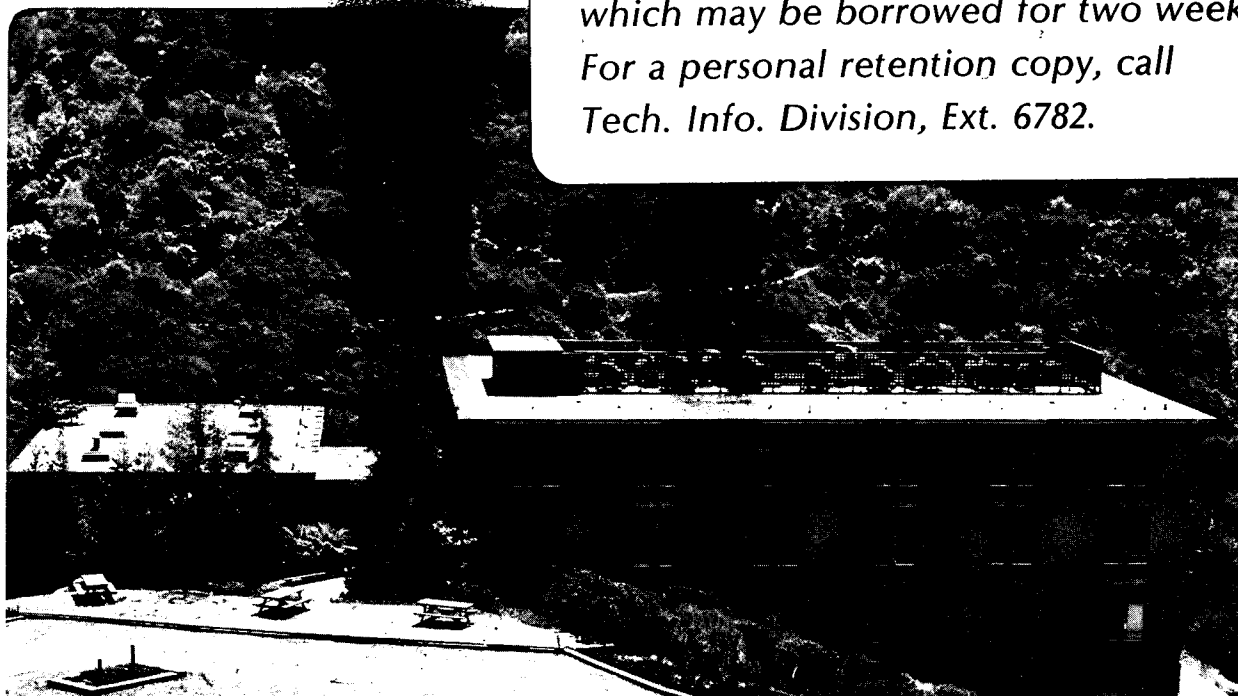
HIGH RESOLUTION MICROSCOPY INVESTIGATION OF THE
ZrO₂ZrN SYSTEM

G. van Tendeloo and G. Thomas

September 1983

TWO-WEEK LOAN COPY

*This is a Library Circulating Copy
which may be borrowed for two weeks.
For a personal retention copy, call
Tech. Info. Division, Ext. 6782.*



LBL-16240
c.2

DISCLAIMER

This document was prepared as an account of work sponsored by the United States Government. While this document is believed to contain correct information, neither the United States Government nor any agency thereof, nor the Regents of the University of California, nor any of their employees, makes any warranty, express or implied, or assumes any legal responsibility for the accuracy, completeness, or usefulness of any information, apparatus, product, or process disclosed, or represents that its use would not infringe privately owned rights. Reference herein to any specific commercial product, process, or service by its trade name, trademark, manufacturer, or otherwise, does not necessarily constitute or imply its endorsement, recommendation, or favoring by the United States Government or any agency thereof, or the Regents of the University of California. The views and opinions of authors expressed herein do not necessarily state or reflect those of the United States Government or any agency thereof or the Regents of the University of California.

High Resolution Microscopy Investigation of the $\text{ZrO}_2\text{-ZrN}$ System⁺

G. van Tendeloo

RUCA, University of Antwerp

Groenenborgerlaan 171

B-2020, Antwerpen, Belgium

and

G. Thomas

Department of Materials Science and Mineral Engineering

and the National Center for Electron Microscopy

Lawrence Berkeley Laboratory

University of California

Berkeley, California 94720, U.S.A.

⁺Paper for the Conference: Zirconia-83, Stuttgart, W. Germany, 1983

Abstract

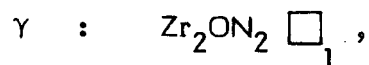
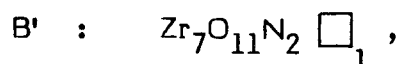
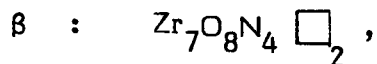
The ZrO_2 -ZrN system has been investigated using different electron microscopy techniques. In the range between 2.5 mol.% and 75 mol.% ZrN, an incommensurate modulated structure is formed having a rhombohedral $R\bar{3}$ symmetry based upon the $\text{Zr}_7\text{O}_{11}\text{N}_2$ structure which is isostructural to $\text{Zr}_5\text{Sc}_2\text{O}_{13}$. The modulation is most probably due to pseudoperiodic composition fluctuations of nitrogen with respect to oxygen. The final structure can be described as a completely coherent mixture of pure Zr_7O_{14} layers alternating with $\text{Zr}_7\text{O}_{11}\text{N}_2$ layers perpendicular to the rhombohedral threefold axis. The incommensurability arises from local deviations in spacing and/or orientation of these layers. Monoclinic precipitates imbedded in this rhombohedral matrix are characterized with the help of high resolution electron microscopy combined with optical microdiffraction.

Introduction

The three polymorphs of ZrO_2 have been well established [1]. At temperatures near the melting point ZrO_2 has the cubic fluorite structure; upon cooling, this structure first undergoes a slight tetragonal distortion and around 1000°C it transforms martensitically towards the monoclinic room temperature phase (spacegroup $P2_1/c$; lattice parameters $a = 0.517$, $b = 0.523$, $c = 0.534\text{nm}$, $\beta = 99^\circ 15'$ [2,3]).

The latter transformation may be completely or partially suppressed by alloying pure zirconia with additions of other oxides such as CaO , MgO or Y_2O_3 [4,5]. The present study is an electron microscopic investigation of a range of ZrO_2 -ZrN alloys in order to investigate a possible stabilisation by ZrN [6] and to elucidate the microstructures.

The formation of different oxynitrides in the Zr-O-N system has been studied by Gilles [7,8]. He established a pseudo binary phase diagram between ZrO_2 and $ZrN_{4/3}$ (not ZrN) and found three structurally related oxynitrides denoted β , β' , and γ with nominal compositions:



where \square denotes a vacancy on the oxynitride sublattice. γ can be described on a cubic lattice with $a = 1.01\text{nm}$, β has a rhombohedral symmetry and is isostructural with $Zr_3Sc_4O_{12}$ or $Zr_3Yb_4O_{12}$ [7]. β' is very closely related to β ; it has also rhombohedral symmetry and the same a -parameter but twice the c -parameter.

Outline of the Investigation

The present investigation refers to materials with the following nominal compositions: $ZrO_2 + 0, 5, 10, 15, 20, 30, 40, 50, 75, 100\%$ ZrN which were investigated "as received" or heat treated at 1000°C . For more experimental details, see [9].

Most of the investigated samples showed a typical morphology as that illustrated in Fig. 1; i.e. large amounts of precipitates embedded in the matrix. From the existing literature, it could be assumed that they were monoclinic ZrO_2 particles in a cubic matrix. However, a closer investigation showed that the matrix was not cubic but rhombohedrally distorted and moreover it showed a complicated incommensurate superstructure [9]. The precipitates were not always monoclinic

but in some cases also tetragonal. The monoclinic precipitates were always heavily twinned. A selected area diffraction pattern (along one of the fluorite cube axes) over such a precipitate is shown as the inset of Fig. 1. Apart from the matrix spots all other reflections can be attributed to different variants of the monoclinic ZrO_2 . From the "conventional" image of Fig. 1, it is impossible to determine twin planes or habit planes. The main aim of the present study was, therefore:

- a) to determine the structure of the matrix
- b) to gain information about the internal structure of the different precipitates.

Structure of the ZrO_2 -ZrN Matrix

(A) Electron Diffraction Evidence

A series of diffraction patterns taken from a matrix area is shown in Fig. 2. From these patterns it can be seen that the structure is not cubic. However, the most intense reflections are close to the cubic fluorite positions, e.g. in Fig. 2f the angle is not exactly 90° but approximately 89° suggesting a rhombohedral distortion. The other diffraction patterns can be divided into two groups:

- (a) reciprocal lattice sections exhibiting a clear superstructure such as $[111]$, $[112]$ or $[103]$ when the fluorite cubic indices are used (Figs. 2a, c and e).
- (b) sections exhibiting extra reflections at incommensurate positions such as $[\bar{1}01]$ and $[\bar{1}\bar{1}2]$ (Figs. 2b,d).

In the $[\bar{3}21]$ cubic section of Fig. 3a, originally cubic reflections are encircled while reflections at commensurate superstructure positions are indicated by

arrows. The remaining reflections are at incommensurate positions but concentrated around commensurate positions such as $(1/2 \ 1/2 \ 1/2)$ which suggests that they might be due to a splitting of a commensurate reflection. The direction of the incommensurate modulation is always along $[111]^*$; i.e. along one of the threefold axes of the originally cubic matrix. The average distance between successive satellites is somewhat variable but always corresponds to a real space periodicity around $3.2 \pm 0.3\text{nm}$.

The commensurate reflections suggest the formation of a superstructure independent of that of the modulation. This becomes evident if one tilts 90° away from the modulation towards a $[111]$ -section (Fig. 2a). The modulation direction is now along the zone axis.

(B) High Resolution Microscopy Evidence

Two essentially different orientations have been examined:

- (a) the $[111]$ zone (perpendicular to the modulation)
- (b) a $[\bar{3}21]$ zone perpendicular to $[111]$, containing the $[111]^*$ row.

In the $[111]$ zone a hexagonal network of bright dots is observed separated by 0.55nm , indicating that the structure has a truly three-fold axis and that the hexagonal pattern of Fig. 2a is not the result of superposition. In the $[\bar{3}21]$ orientation a modulated structure with a periodicity of about 3nm can be easily recognised. The modulation is not exactly periodic and in some areas spacing, as well as orientation deviations can be observed. At a higher magnification (Fig. 4), it becomes evident that the modulation is not of the interface modulated kind. There is no well defined defect plane; the image appears more like a sinusoidal intensity modulation. However, when observed along the $[1\bar{1}5]_{\text{cub}}$ direction (e.g. in Fig. 4) a shift in intensity maxima is observed between subsequent modulations, separated by 3nm .

In very restricted areas, mostly close to a monoclinic precipitate, the unmodulated structure is observed (Fig. 4a, left side) in contact with the modulated structure (Fig. 4a, right side). Since the areas are too small for conventional electron diffraction and since convergent beam diffraction is too difficult due to beam damage which causes the superstructure to disappear, selected area laser optical diffraction from the matrix as well as from the modulated structure were used (Figs. 4b, c). They prove that both structures are closely related and that some reflections which are unsplit in the commensurate superstructure such as (1/2 1/2 1/2) are split up into different satellites due to the modulation.

(C) Structure of the Unmodulated Phase

Assuming, as evidenced from Fig. 2f, that the structure is a slight rhombohedral modification of the fluorite type structure and taking into account the doubling of the periodicity along this rhombohedral axis (Fig. 4b), the unit cell parameter along the \bar{c} -axis should be around 1.8nm (assuming a hexagonal description of the rhombohedral structure). This would fit excellently with the β' phase described by Gilles [7] which seems to be isostructural to $Zr_5Sc_2O_{13}$ [10]. More details can be found in [9]. The measured unit cell parameters are $a = 0.96\text{nm}$ and $c = 1.76\text{nm}$ and the complete relation between fluorite structure $(\bar{a}_1, \bar{a}_2, \bar{a}_3)$ and the superstructure $(\bar{A}_1, \bar{A}_2, \bar{A}_3)$, when omitting the rhombohedral distortion, can be derived from the diffraction patterns to be:

$$\begin{bmatrix} \bar{A}_1 \\ \bar{A}_2 \\ \bar{A}_3 \end{bmatrix} = \begin{bmatrix} 1 & -3/2 & 1/2 \\ 1/2 & 1 & -3/2 \\ 2 & 2 & 2 \end{bmatrix} \begin{bmatrix} \bar{a}_1 \\ \bar{a}_2 \\ \bar{a}_3 \end{bmatrix}$$

In the cubic fluorite structure, every Zr-atom is surrounded by 8 oxygens and the structure can be described as built up from ZrO_8 cubes sharing edges with each other [9,10]. When the anion to cation ratio deviates from the ideal value of two (e.g. in $Zr_5Sc_2O_{13}$ or $Zr_3Sc_4O_{12}$) vacancies are introduced and some of the cations only have a 6-fold or a 7-fold coordination. The basic building block turns out to be the so-called "Bevan cluster" [11] represented in Fig. 5. It consists of a sixfold coordinated metal atom (hatched cube) surrounded by six sevenfold coordinated cubes sharing edges with the central cube. Both vacancies in this cluster necessarily are at diagonally opposite sites of the central cube in order to retain the rhombohedral threefold symmetry along [111]. The β -phase $Zr_7O_8N_4$ \square_2 is exclusively built up by stacking layers of such clusters perpendicular to the threefold axis while the β' phase $Zr_7O_{11}N_2$ \square_1 (isostructural to $Zr_5Sc_2O_{13}$) would be built up by an equal amount of layers of such Bevan clusters and layers of "ideal" clusters where all metal atoms have an eightfold coordination. In this sense the β' phase can be considered as intermediate between the cubic fluorite phase and the β -phase. The cubic fluorite as well as the β -phase has a three layer periodicity along $[111]_{cub}$ or $[0001]_{hex}$; the first one is completely built up from perfect I (ideal) clusters while the second is completely built up from B (Bevan) clusters, all oriented along the unique threefold axis. The β' phase having a six layer periodicity is a mixture of equal amounts of B and I cluster layers such that the structure can be written as BIBIBI while the β phase is BBB and the cubic ZrO_2 phase is III.

(D) Structure of the Modulated Phase

Analysis of the modulated structure must take into consideration the following experimental data:

- it is a modulation of the rhombohedral β' $Zr_7O_{11}N_2$ structure;
- the modulations are roughly parallel to $(00.1)_{\beta}$ with an average distance of 3.2nm but not strictly bound to this plane;
- the high resolution microscopy shows a modulation which is not of the interface modulated type (e.g. different from long period superstructures) but after one wavelength an out of phase shift is observed (Fig. 4).

With knowledge of the basic β' structure and from the shift of the satellites with respect to their original position, one can obtain more information about this last point. Indeed, although there is no discrete interface visible in the high resolution micrographs, the boundary can be described as in Fig. 6a, which is in fact the same as the purely interface modulated structure (e.g. for a long period antiphase boundary structure) (Fig. 6b) except for the fact that the boundary is smeared out. The final displacement, however, between A and B is the same as that between A' and B'. Neglecting the reason for the origin for such a smeared out interface, one can determine the displacement vector \bar{R} for this boundary in the same way as one can do for periodic antiphase boundaries or shear planes [12].

Careful inspection of the diffraction patterns shows that all satellites undergo a shift which is 0 (mod 1) or 1/2 with respect to the β' positions. From the shift of three independent reflections the displacement vector can be determined as:

$$\bar{R} = \pm [2/3 \ 1/3 \ 1/6] ;$$

Since the \bar{R} vector is not in the defect plane, this displacement is non-conservative and implies a deviation from ideal stoichiometry.

The high resolution observations (Fig. 4) indicate that the modulation has more of a wave character than an antiphase character. Similar considerations have been made for (Au,Ag)Te₂ [13], Mo_{2+x}S₃ [14] and the "chimney ladder" structure in MnSi_{2-x} [15].

Precipitation in the Rhombohedral Zr-O-N Matrix

Precipitation in the rhombohedral Zr-O-N matrix is a complex phenomenon. Tetragonal as well as monoclinic ZrO₂ particles can be present in the matrix [9].

In this summary only the monoclinic precipitation is considered; internal twinning occurs frequently in these precipitates and based on the type of twinning, two essentially different twin structures can be considered:

- (a) precipitates with all twin variants having a common \bar{c} -axis;
- (b) precipitates with twin variants having no common axis.

A high resolution example of the first type is shown in Fig. 7 when viewed along the c_m axis. The precipitate is heavily twinned and all twin boundaries are edge on, and strictly along crystallographic planes. Such configurations are very similar to the ones observed by Kriven for 50% Al₃O₂ - 50% ZrO₂ [16] and for ZrO₂ particles in a mullite matrix [17]. The frequent and almost regular (100) twinning of such precipitates occurs to minimize strain and shape deformation effects built up as a result of the differences in lattice parameters due to the monoclinic shear transformation.

The second type of precipitate is more complex and produces diffraction patterns (insert, Fig. 1) which are very complex. High resolution microscopy combined with optical diffraction seems to be the only way to correlate the different diffraction spots with areas in direct space. The usual dark field technique, i.e. selecting successively all diffracted reflections to form an image, fails in this case

because the reflections are too close to each other to be individually imaged. The lattice image (Fig. 8a, b) establishes the presence of six different orientation variants and with the aid of optical diffraction over the different domains (bottom), one can deduce the orientation relationship as indicated in Fig. 8b.

Conclusions

High resolution electron microscopy combined with electron diffraction and laser optical microdiffraction has been shown to be a powerful technique to interpret the complex microstructures obtained in alloys of ZrO_2 -ZrN. These complexities include the formation of an incommensurate modulated rhombohedral matrix containing twinned ZrO_2 precipitates. The easy beam damage to these materials means that high voltage microscopy is essential. Microchemical analyses at 100kV using EELS for mapping oxygen and nitrogen is almost impossible [18].

Acknowledgements

This work was supported by the Director, Office of Energy Research, Office of Basic Energy Sciences, Materials Sciences Division of the U. S. Department of Energy under Contract No. DE-AC03-76SF00098. The authors are grateful to L. Anders for preparing electron microscopy samples. Financial support has been provided by the NSF. One of us (G.V.T.) is also indebted to NATO for partial financial support. We also thank Drs. S. Amelinckx, U. Dahmen, R. Gronsky and A. H. Heuer for valuable discussions.

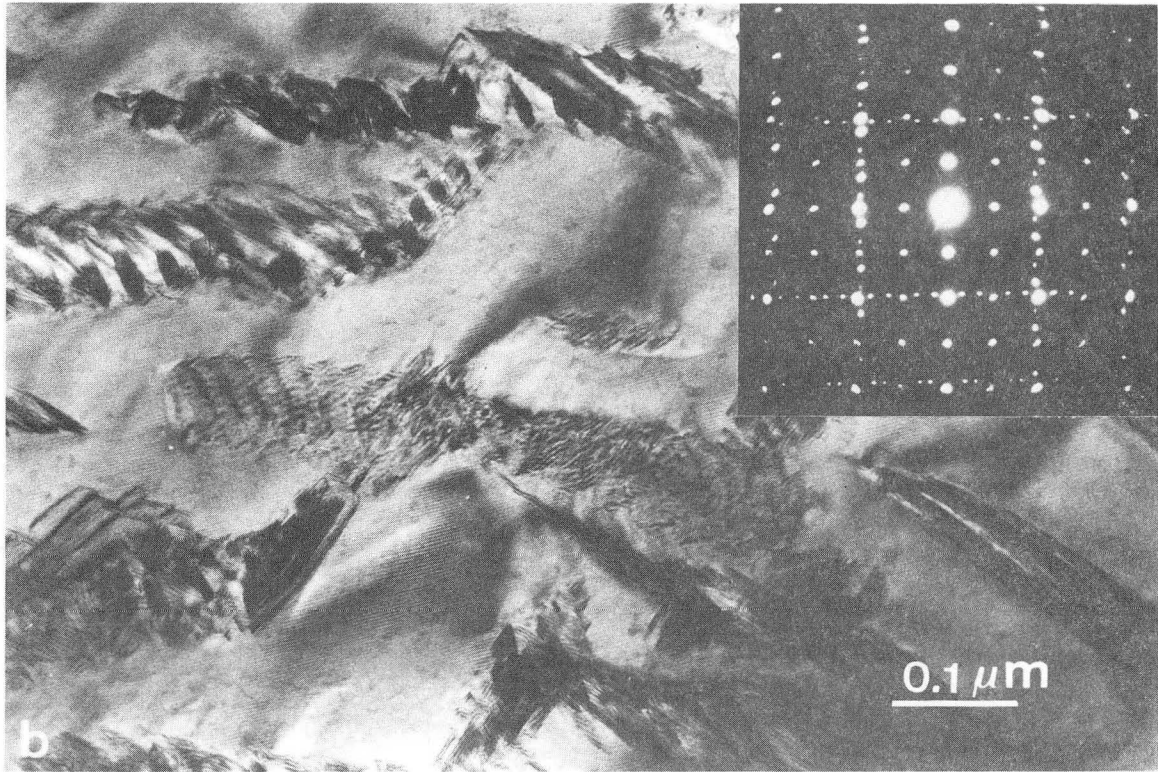
References

1. E. C. Subbarao, *Advances in Ceramics* 3, 1 (1981), eds. A. H. Heuer and L. W. Hobbs, Columbus, Ohio.
2. J. D. McCullough and K. N. Trueblood, *Acta Cryst.* 12, 507 (1959).
3. D. K. Smith and H. W. Newkirk, *Acta Cryst.* 18, 983 (1965).
4. V. S. Stubican and J. R. Hellman, *Advances in Ceramics* 3, 25 (1981).
5. D. L. Porter and A. H. Heuer, *J. Am. Ceram. Soc.* 62, 298 (1979).
6. A. Claussen, R. Wagner, L. J. Gauckler and G. Petzow, *J. Am. Ceram. Soc.* 61, 369 (1978).
7. J.-C. Gilles, *Rev. Hautes Temp. et Refract.* 2, 237 (1965).
8. J.-C. Gilles and R. Collongues, *C. R. Acad. Sci. Paris* 254, 1084 (1962).
9. G. van Tendeloo and G. Thomas, *Acta Met.* (1983), parts I and II, in press.
10. M. R. Thornber, D. J. M. Bevan, and J. Graham, *Acta Cryst.* B24, 1183 (1968).
11. B. Hudson and P. T. Moseley, *J. Sol. State Chem.* 19, 383 (1976).
12. J. Van Landuyt, R. De Ridder, R. Gevers, and S. Amelinckx, *Mat. Res. Bull.* 5, 353 (1970). Also see R. De Ridder, J. Van Landuyt, and S. Amelinckx, *phys. stat. sol. (a)* 9, 551 (1972).
13. G. van Tendeloo, P. Gregoriades and S. Amelinckx, *J. Sol. State Chem.* in press, (1983).
14. R. Deblieck, G. A. Wieggers, K. D. Bronsema, D. Van Dyck, G. Van Tendeloo, J. Van Landuyt and S. Amelinckx, *phys. stat. sol. (a)* 77, 249 (1983).
15. R. De Ridder, G. van Tendeloo and S. Amelinckx, *phys. stat. sol. (a)* 33, 383 (1976).
16. W. M. Kriven, in *Advances in Ceramics* 3, 168 (1981), eds. A. H. Heuer and L. W. Hobbs, Columbus, Ohio.

17. E. Bischoff and M. Rühle, J. Am. Ceram. Soc. 66, 123 (1983).
18. M. Sarikaya, P. Rez and G. Thomas, to be published.

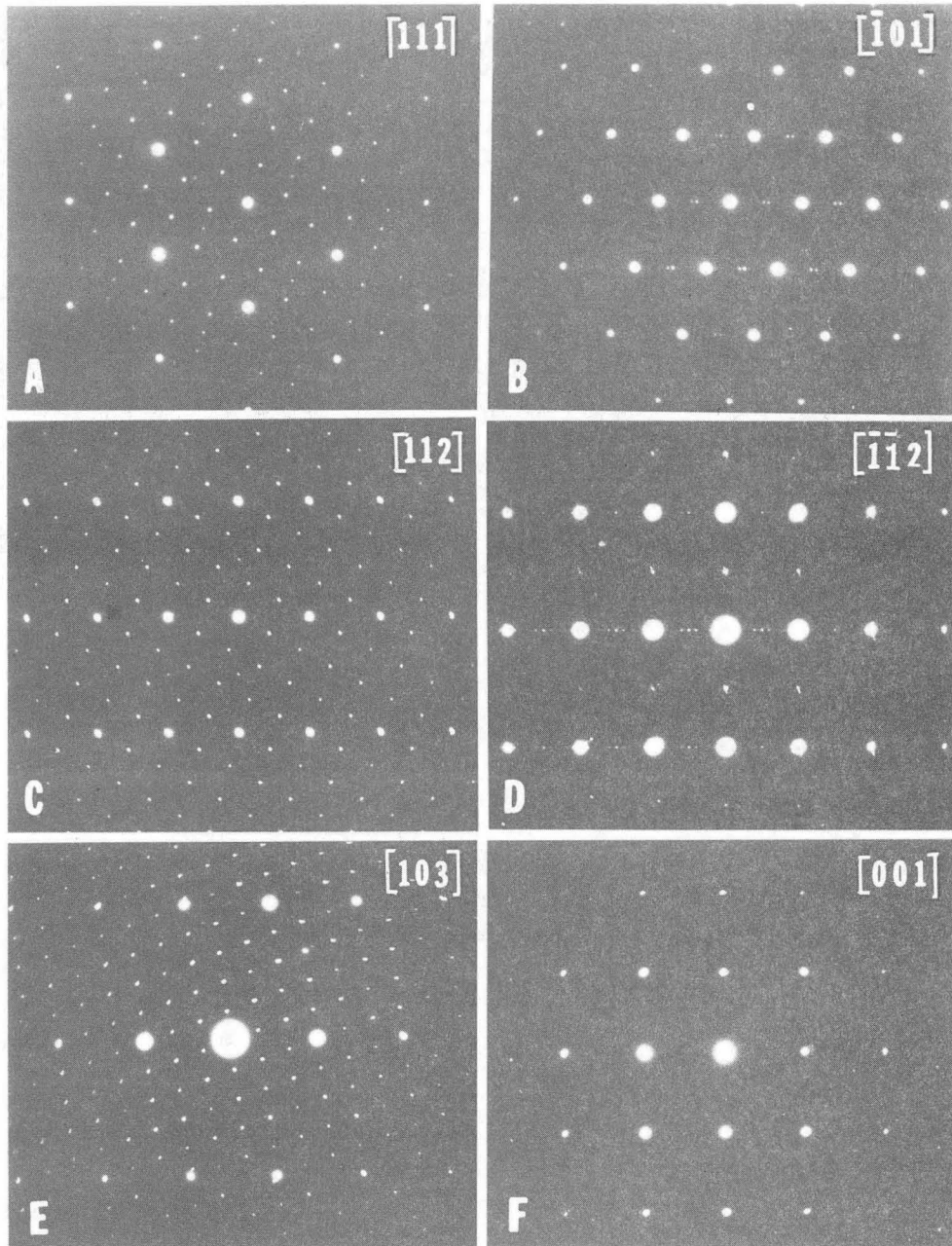
Figure Captions

- Fig. 1a Typical morphology of most $\text{ZrO}_2\text{-ZrN}$ samples. The electron diffraction pattern over a precipitate is shown as an inset.
- Fig. 2 Diffraction series taken from Zr-O-N matrix.
- Fig. 3a $[\bar{3}21]_{\text{cub}}$ diffraction pattern; cubic reflections are indicated by dots, commensurate superstructure reflections are indicated by arrows.
- Fig. 3b High resolution image corresponding to Fig. 3a. Note the orientation deviations at the lower right corner.
- Fig. 4a High resolution image of the basic superstructure in contact with the modulated structure. The orientation is $[\bar{3}21]_{\text{cub}}$. (see Fig. 3a)
- Fig. 4b,c Laser optical microdiffraction pattern from the unmodulated (b) as well as from the modulated (c) structure.
- Fig. 5 The Bevan cluster, consisting of seven cubes; the center of each cube contains a Zr atom. The central Zr has a sixfold coordination ZrO_6 while all other Zr atoms have a sevenfold coordination ZrO_7 .
- Fig. 6 Schematic representation of (a) wavy modulation compared to a strict long period interface modulated structure (b).
- Fig. 7 High resolution observation of heavily twinned monoclinic ZrO_2 . All variants have a common c-axis parallel to the electron beam. The orientation of the axes as determined from HREM and optical diffraction is indicated.
- Fig. 8 A complex twinned area analysed with the aid of high resolution microscopy and laser optical diffraction of the areas indicated 3-6.



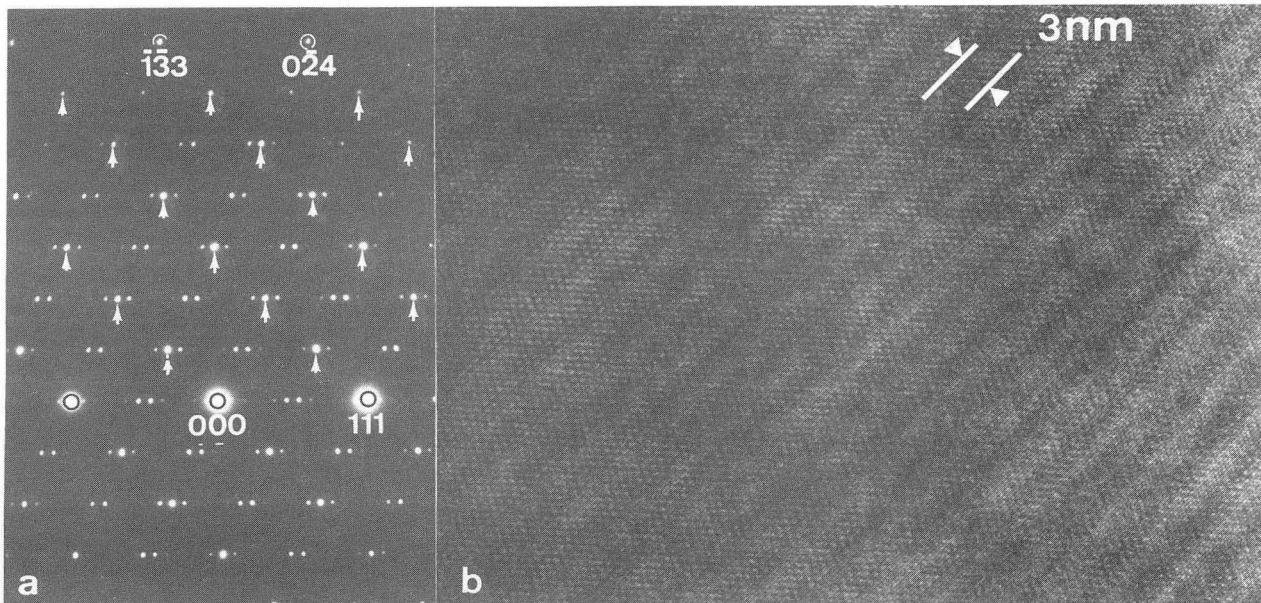
XBB 838-7150

Fig. 1



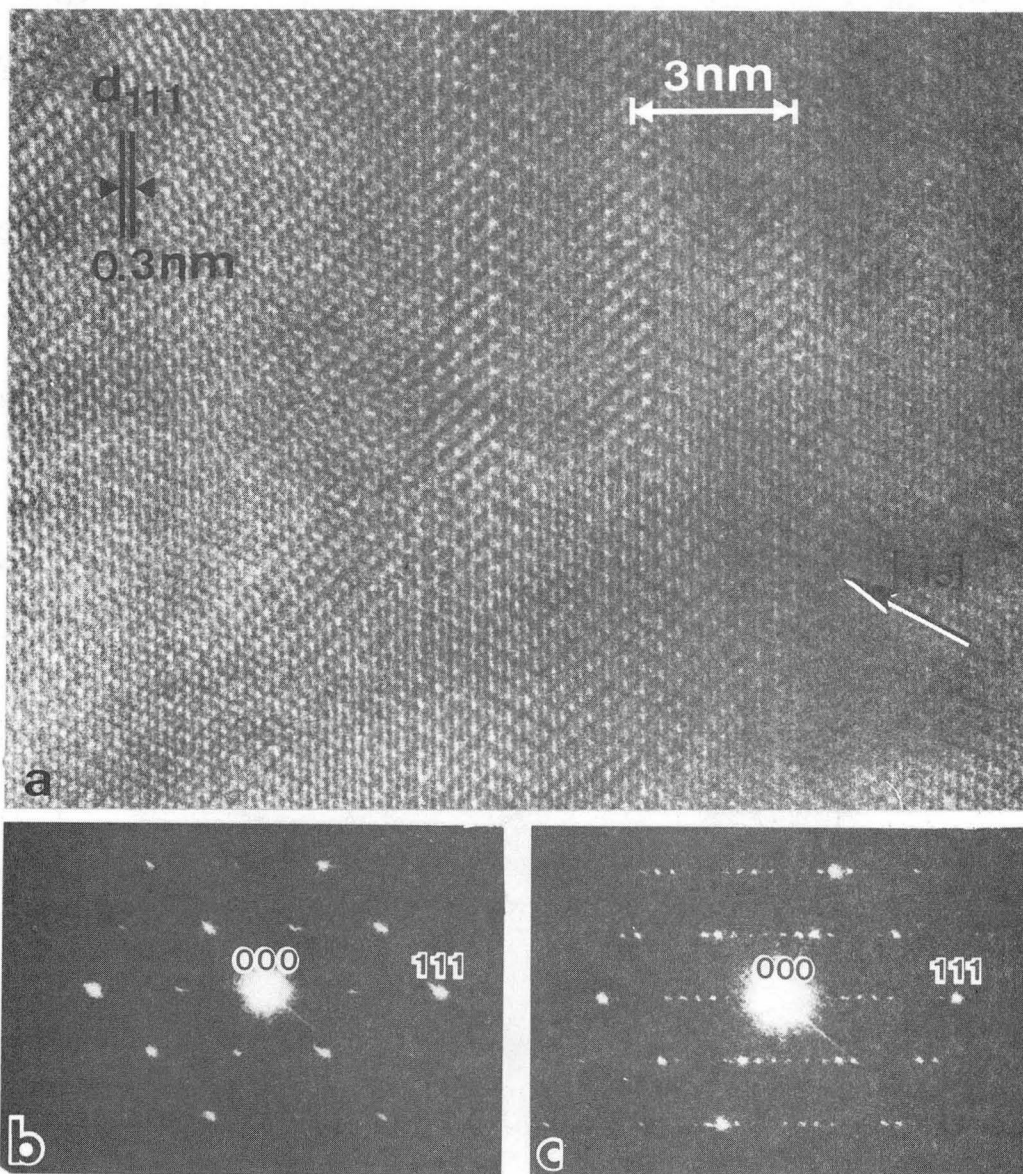
XDB 838-7151

Fig. 2



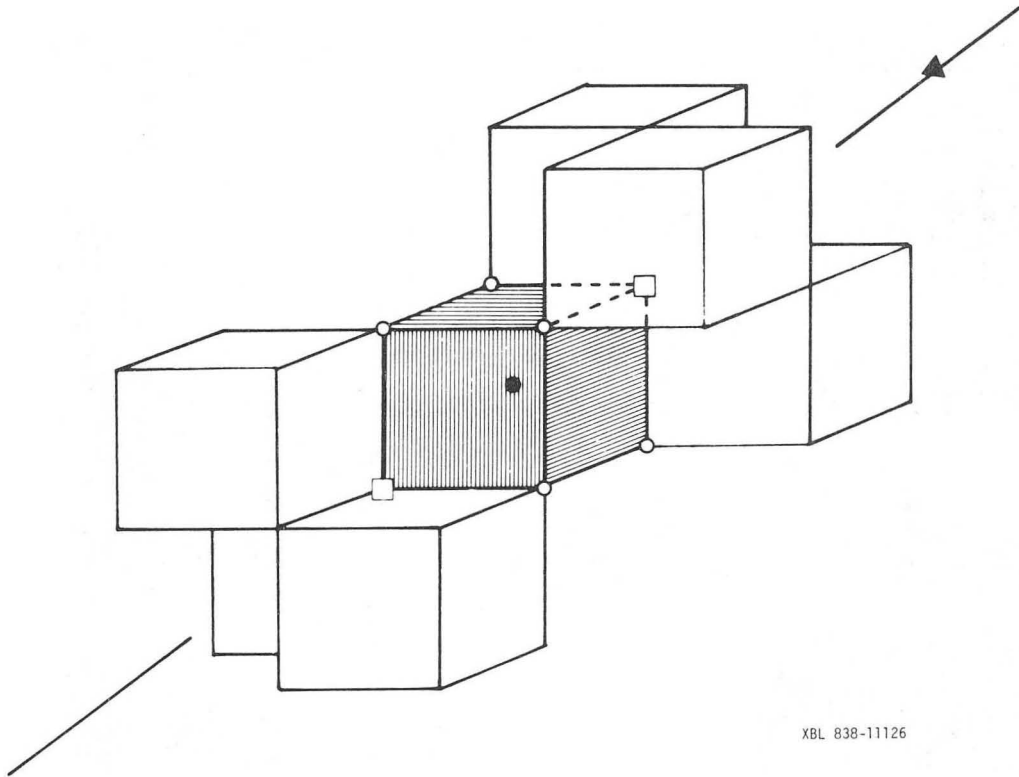
XBD 838-7153

Fig. 3



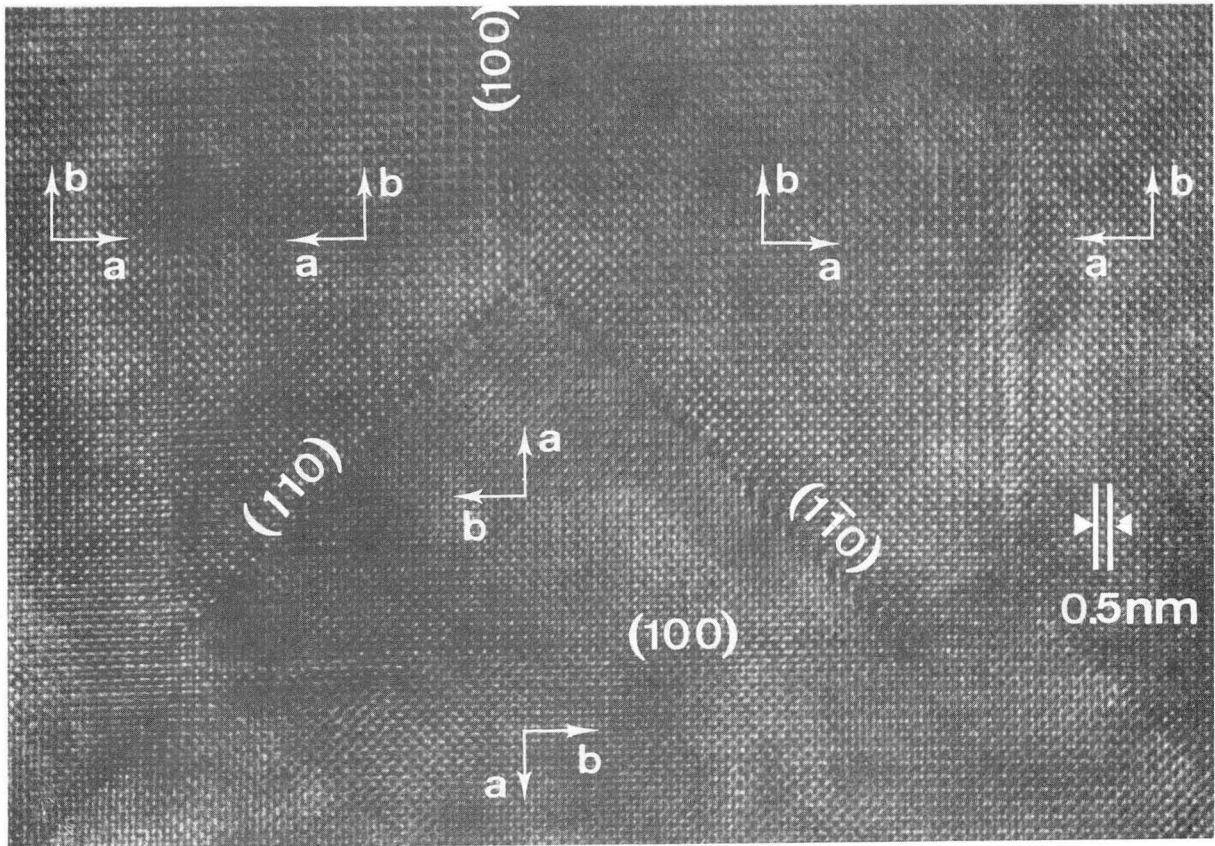
XBB 838-7154

Fig. 4



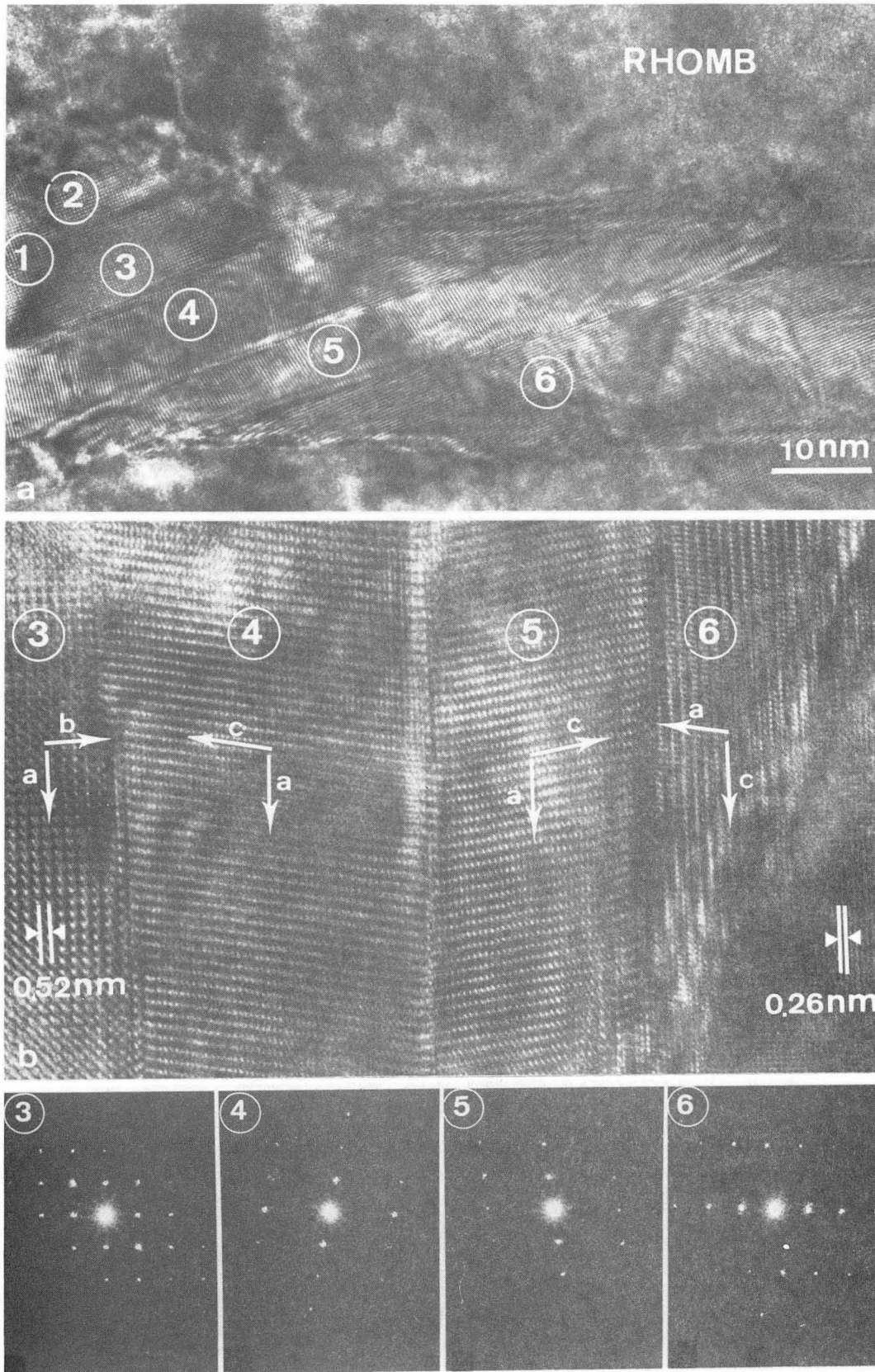
XBL 838-11126

Fig. 5



XBB 838-7156

Fig. 7



XDB 838-7159

Fig. 8

This report was done with support from the Department of Energy. Any conclusions or opinions expressed in this report represent solely those of the author(s) and not necessarily those of The Regents of the University of California, the Lawrence Berkeley Laboratory or the Department of Energy.

Reference to a company or product name does not imply approval or recommendation of the product by the University of California or the U.S. Department of Energy to the exclusion of others that may be suitable.

TECHNICAL INFORMATION DEPARTMENT
LAWRENCE BERKELEY LABORATORY
UNIVERSITY OF CALIFORNIA
BERKELEY, CALIFORNIA 94720